ORGANOMETALLICS

pubs.acs.org/Organometallics Article

Lewis Base Activation by Uranium(III) Complexes

Nathan J. Lin, Diana Perales, Ellen M. Matson, Matthias Zeller, and Suzanne C. Bart*

Cite This: *Organometallics* 2023, 42, 641−650 Read Online

ACCESS | Metrics & More | Article Recommendations | Supporting Information

ABSTRACT: The combination of a bulky hypersilyl potassium [$(Me_3Si)_3SiK$] reagent with Tp^*_2UI (Tp^* = hydrotris(3,5-dimethylpyrazolyl)borate) in the presence of ethereal Lewis donors resulted in the formation of base-activated products $Tp^*_2U[O(CH_2)_4Si(SiMe_3)_3]$ (**1-THF**) and $Tp^*_2U[O(CH_2)_2OMe]$ (**2-DME**). The reactivity with another Lewis base, pyridine, was explored by treating Tp^*_2UI and hypersilyl potassium or benzyl potassium in the presence of pyridine, which resulted in formation of $Tp^*_2U[NC_5H_5\text{-}4\text{-}Si(SiMe_3)_3]$ (**3-py-Si**) and $Tp^*_2U(NC_5H_5\text{-}4\text{-}Bn)$ (**4-py-Bn**, Bn = benzyl), respectively. Multinuclear paramagnetic NMR spectroscopy (^1H, $^{11}B\{^1H\}$, $^{29}Si\{^1H\}$) supported the formation of the Lewis base activated uranium compounds as corroborated by electronic absorption spectroscopy and X-ray crystallography. To recognize the mechanistic possibilities, radical trap experiments were performed and [K(18-crown-6)][4-benzylpyridinide] (**4-K**), Tp*U(IV)[(=NC(Me)C(H)C(Me)N)-B(H)(3,5-dimethylpyrazole)$_2$] (**6-Tp*UTp′**), and $[Tp^*_2U(NC_5H_5)]_2$ (**5-py-py**) were observed.

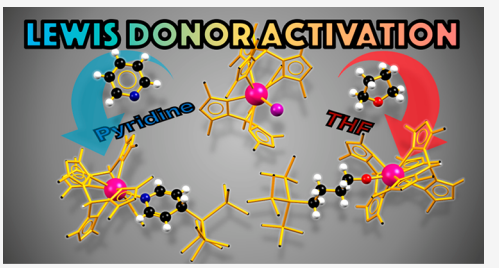

INTRODUCTION

To combat contamination in the environment from increasing amounts of spent nuclear fuel storage, an interest in fundamental actinide coordination chemistry has grown in recent years.[1−3] Given that uranium is the major component of these mixtures, understanding small molecule reactivity with this metal ion is essential.[4] Equally paramount is understanding how actinide compounds interact with polar Lewis bases, such as organic solvents, for applications in separations of spent nuclear waste.[5,6]

Lewis basic solvents play an essential role in the electronic and steric saturation for low-valent actinide complexes.[7,8] In 1983, Sattelberger et al. reported the stability of UI_3 adducts with a wide range of Lewis bases including tetrahydrofuran (THF), 1,2-dimethoxyethane (DME), and pyridine;[9] in some cases of tetravalent uranium, however, THF was discovered to undergo ring-opening.[10−12] Gambarotta and co-workers have shown that even stronger C−O bonds in ethereal solvents, such as DME, can be broken in both one and two electron pathways in the presence of electron rich Th centers.[13]

Other electron-rich actinide complexes have also been shown to activate Lewis bases, including pyridine. The Mazzanti and Mills groups found that introduction of pyridine to "masked U(II)" and Th(III) complexes generates $[((Me_3Si)_2N)_3U(III)\}_2\{\mu\text{-}(NC_5H_5)_2\}]$ and $[\{Th(IV)\text{-}(Cp'')_3\}_2\{\mu\text{-}(NC_5H_5)_2\}]$ [Cp′′ = 1,3-di(trimethylsilyl)-cyclopentadienyl] dimers, respectively.[14,15] These dimers have been proposed to form from a reduced metal-bound pyridine radical. Activated pyridine complexes have also been observed in transition metal systems and can activate reactive species in solution.[15−19]

Our group has demonstrated that the bulky hydrotris(3,5-dimethylpyrazolyl)borate (Tp^*) ligand can stabilize a wide variety of low-valent uranium complexes including alkyls,[20] oxos,[21] imides,[22−24] and recently, bonds to heavier main group elements.[25] Previous work from our group has also shown the activation of substituted triphenylphosphine oxides by a family of uranium(III) alkyl complexes supported by the bis-Tp^* framework,[26] demonstrating Lewis base activation by the highly reducing alkyl substituent. Similarly, we recently reported the ring-opening of THF by U−P bonds in the $Tp^*_2U\text{−}PHR$ (R = Ph, Mes, Mes*; Mes = 2,4,6-trimethylphenyl; Mes* = 2,4,6-tri-*t*Bu-phenyl) family.[25]

Missing in the repertoire of bis-Tp^* uranium complexes is the U−Si bond. Although U−Si bonds, including U(IV)−$Si(SiMe_3)_3$, exist in the literature,[27,28] only recently have silyl bonds been observed for a uranium(III) center.[29] In attempts to expand the library of U(III)−Si bonds by treating Tp^*_2UI with $(Me_3Si)_3SiK$,[30] it was discovered that the base-stabilized U−Si bond was not observed using the Tp^* scaffold, but instead a variety of base-activated products are isolated. These derivatives were fully characterized using multinuclear NMR, electronic absorption, and IR spectroscopies, as well as X-ray crystallography in cases where suitable single crystals were obtainable. The reactivity and potential mechanistic pathways for these base-activated complexes are discussed.

Received: December 20, 2022
Published: April 10, 2023

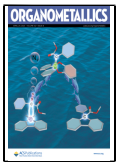

https://doi.org/10.1021/acs.organomet.2c00633
Organometallics 2023, 42, 641−650

RESULTS AND DISCUSSION

THF and DME as Lewis Bases. Dropwise addition of a toluene solution of $(Me_3Si)_3SiK{\cdot}2THF$ into a solution of Tp^*_2UI at −35 °C produced a brown, pentane-soluble powder upon workup (Scheme 1). ^1H NMR spectroscopy in C_6D_6

Scheme 1

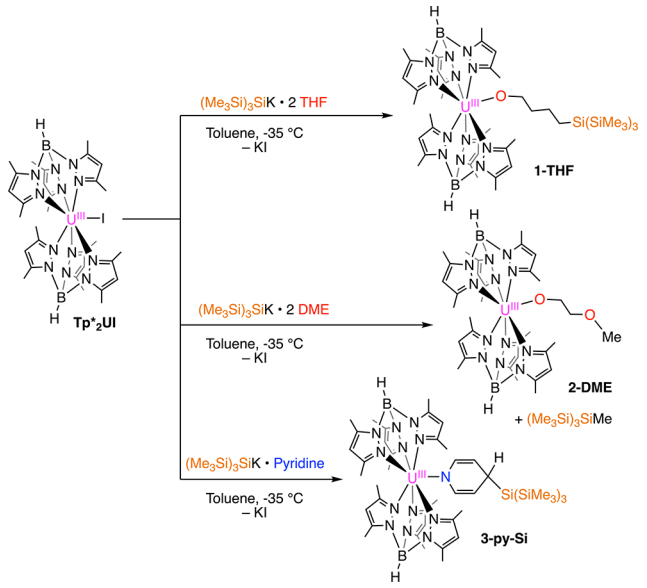

showed a singlet at 3.9 ppm, which was assigned as the nine equivalent methyl groups of the hypersilyl moiety (27 H), as well as broad resonances at 13.7, 22.6, 43.03, and 103.4 ppm, which were hypothesized to originate from ring-opened THF. To confirm this, the synthesis was repeated with $(Me_3Si)_3SiK{\cdot}2THF\text{-}d_8$, which identified the ring-opened THF CH_2/CD_2 resonances to be those listed above by their absence in the ^1H NMR spectrum. In addition, the $^{11}B\{^1H\}$ NMR signal at −7.7 ppm indicates a U(III) ion due to similarity in the $^{11}B\{^1H\}$ NMR chemical shift to other bis-Tp* U(III) compounds.[23] The $^{11}B\{^1H\}$ NMR chemical shift for bis-Tp^*_2U(III) complexes typically lies within the range of −20 to 10 ppm, while bis-Tp^*_2U(IV) complexes typically resonate between −60 to −80 ppm. The $^{29}Si\{^1H\}$ NMR spectrum shows two clear resonances at −8.6 and −75.0 ppm, assigned as the $\underline{(Me_3Si)_3}Si$ and the $(Me_3Si)_3\underline{Si}$ atoms, respectively, with the latter much further shifted from a known uranium-bound silicon atom (−137 ppm) and not representative of free ligand [$(Me_3Si)_3SiK$ = −4.55, −194.10 ppm].[27] These multinuclear NMR data suggested THF activation and formation of $Tp^*_2U[O(CH_2)_4Si(SiMe_3)_3]$ (**1-THF**) (Scheme 1).

To circumvent ring opening of THF, DME was used instead. The addition of $(Me_3Si)_3SiK{\cdot}2DME$ to Tp^*_2UI generated a brown solution that gave a ^1H NMR spectrum similar to that of **1-THF**, but with slight shifts in the paramagnetic region. The ^1H NMR spectrum of the reaction mixture revealed a large $(Me_3Si)_3Si$ resonance at 0.27 ppm. In addition, the elucidation of two signals at −13.0 and −88.4 ppm in the $^{29}Si\{^1H\}$ NMR spectrum indicated that $(Me_3Si)_3SiMe$[31] is the byproduct of the reaction, suggesting the formation of isolable $Tp^*_2U[O(CH)_2OMe]$ (**2-DME**) (Scheme 1) and demonstrating a rare silyl transfer to a methyl group.

The B−H stretches in the infrared region for **1-THF** and **2-DME** range from 2529 to 2562 cm^{-1} and are typical for bis-Tp* uranium complexes.[20,22,23] The large bands from 1200 and 1191 cm^{-1}, respectively, are suggested to be the wagging modes of the alkoxide chain.[11]

These compounds were analyzed by electronic absorption spectroscopy from 200 to 1600 nm in THF at ambient temperature. The brown color of **1-THF** and **2-DME** is likely due to the intense absorption bands between 350 and 500 nm in the UV−visible region (Figure S31). The NIR region for **1-THF** and **2-DME** shows typical *f*−*f* transitions between 1150 to 1400 nm, consistent with a U(III) oxidation state (Figure S31).[22,23]

Collection and refinement of single crystal X-ray diffraction data from the two crystalline products confirmed the generation of alkoxides **1-THF** and **2-DME** (Figure 1). Both

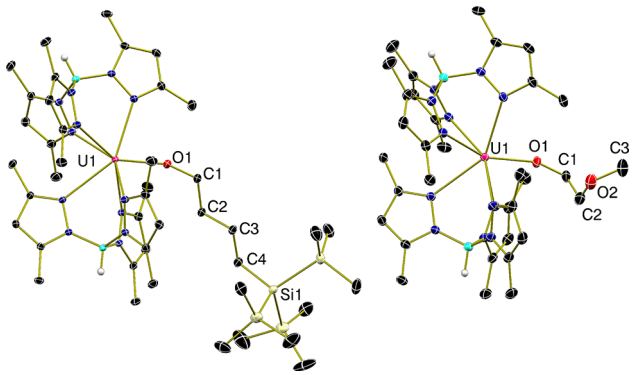

Figure 1. Molecular structures of **1-THF** (left) and **2-DME** (right) displayed with 30% probability ellipsoids. Selected hydrogen atoms and minor disordered moieties were omitted for clarity.

uranium ions in **1-THF** and **2-DME** are distorted capped trigonal prisms. The $U{-}N_{pyrazole}$ distances in **1-THF** and **2-DME** are roughly equivalent, ranging from 2.5509(11)−2.7255(11) Å and 2.527(2)−2.7723(19) Å, respectively. The U−O distance of 2.1497(10) Å in **1-THF** and 2.144(7)−2.29(2) Å in **2-DME** are similar to that of a known bis-Tp* U(III) aryloxide compound (2.159(10) Å).[12,32] In contrast, the U(IV)−O distances in bis-Tp U(IV) (Tp = hydrotris(pyrazolyl)borate) alkoxide compounds are much shorter (2.012(14)−2.028(9) Å).[12]

Definitive structural analysis of **1-THF** and **2-DME** indicates that uranium(III) in the presence of $(Me_3Si)_3SiK$ with ethereal donors induces C−O cleavage, forming stable U(III) aryloxide compounds. To determine if the high oxophilicity of uranium was the culprit of these transformations, pyridine was used as the stabilizing solvent donor.

Pyridine as the Lewis Base. The addition of $(Me_3Si)_3SiK{\cdot}$pyridine to a toluene mixture of Tp^*_2UI at −35 °C resulted in a blue-green solution. The ^1H NMR spectrum of this compound in C_6D_6 showed full consumption of starting materials as well as five new paramagnetic resonances. The largest resonance at 5.1 ppm was assigned as the nine symmetric methyl groups of the hypersilyl group for this new product, which is similar in chemical shift to that of **1-THF**. The ^1H NMR spectrum also revealed multiple small resonances in a similar region to those found in **1-THF** and **2-DME**, suggesting activation of the solvent. The addition of pyridine-d_5 to a solution of $(Me_3Si)_3SiK{\cdot}2THF$ was used in a parallel experiment to identify the activated pyridine in the ^1H

https://doi.org/10.1021/acs.organomet.2c00633
Organometallics 2023, 42, 641−650

NMR spectrum of this paramagnetic product (Figure S13). Doing so revealed that resonances at 22.2, 32.7, and a broad resonance at 44 ppm originated from the pyridine moiety. The presence of three resonances instead of four indicated that the silyl group is bound to the 4-position and suggested the formation of $Tp^*_2U[NC_5H_5\text{-}4\text{-}Si(SiMe_3)_3]$ (**3-py-Si**, Scheme 1).

To confirm the oxidation state, the $^{11}B\{^1H\}$ NMR spectrum was collected and a broad signal corresponding to the B−H proton on Tp* at −9.9 ppm suggested a U(III) ion within the bis-Tp* manifold.[22] A broad resonance at −2.4 ppm in the ^1H NMR spectrum also corroborated conservation of a Tp* uranium species, despite the lack of 3,5-dimethylpyrazolyl resonances.[25]

In **3-py-Si**, the $^{29}Si\{^1H\}$ NMR spectrum contains a signal at −6.8 ppm for the $\underline{(Me_3Si)_3}Si$ atom as well as a signal at −51.0 ppm for the $(Me_3Si)_3\underline{Si}$ atom. As a comparison from a direct U(IV)−$Si(SiMe_3)_3$ interaction [$\underline{(Me_3Si)_3}Si$: −9.83, $(Me_3Si)_3\underline{Si}$: −137.09 ppm], **1-THF** and **3-py-Si** are not as influenced by paramagnetic spin−orbit coupling[33,34] as indicated by the shift differences of the $(Me_3Si)_3\underline{Si}$ atom. In addition, **1-THF** and **2-DME** also resonate outside the tabulated range of other silicon-containing U(III) compounds (−116 to −247 ppm).[35] The reasoning for both is likely due to the five- to six-bond distance from the U(III) center to the nearest silicon atom.

Repeating the synthesis of **3-py-Si** with pyridine as a solvent did not result in a clean product but rather a dark brown-green solution. ^1H NMR analysis made it possible to identify **3-py-Si**, but this was intractable from other impurities identified as $Tp^*_2U(dmpz)$ (dmpz = 3, 5-dimethylpyrazolate)[32] and organosilicon byproducts. In addition, a solution of $(Me_3Si)_3SiK$ dissolved in toluene with equimolar 1:1 THF/pyridine or 1:1 DME/pyridine when added to Tp^*_2UI resulted in formation of **3-py-Si** as the product along with some unidentified impurities. The result of this competition experiment establishes pyridine's strength as a Lewis base when compared to both THF and DME, as previously reported.[36] Although uranium is known for its oxophilicity, it is apparent here that pyridine is preferred in competition with THF or DME due to not only pyridine's Lewis basic strength, but also its proclivity for reduction and ability to undergo nucleophilic attack.

This phenomenon of pyridine activation was also encountered as previously unpublished results from our group with Tp^*_2UBn[20,23] (Bn = benzyl). However, Tp^*_2UBn represents a convenient system for studying pyridine activation within the context of our ligand system in depth. Tp^*_2UBn is traditionally synthesized by addition of KBn to Tp^*_2UI in THF without the activation of the solvent demonstrating that this uranium compound is not oxophilic enough to react with ethereal solvents (Scheme 2).[20] However, with the addition of pyridine to Tp^*_2UBn, formation of a blue-green product was observed. As studied through NMR spectroscopy, the same blue-green product was observed through an alternate synthesis of Tp^*_2UI and KBn in pyridine.

In both cases, the ^1H NMR spectra showed seven paramagnetically shifted resonances between 9.4 and 42.6 ppm. The symmetric solution structure suggests the activation of pyridine exclusively in the 4-position, which is likely sterically driven by the bulky Tp* ligand (as opposed to the asymmetric 2-positional isomer). These ^1H NMR spectroscopic data suggest formation of $Tp^*_2U(NC_5H_5\text{-}4\text{-}Bn)$ (**4-py-Bn**, Scheme 2) and demonstrate a noteworthy account of 1,4-addition of pyridine to a U−C bond. However, we were interested in further NMR characterization of this complex due to the absence of 3,5-dimethylpyrazolyl resonances from Tp* which is a phenomenon not commonly observed with other U(III) bis-Tp* complexes. ^2H and ^1H−^1H COSY NMR techniques were employed to confirm the solution structure of **4-py-Bn**.

Scheme 2

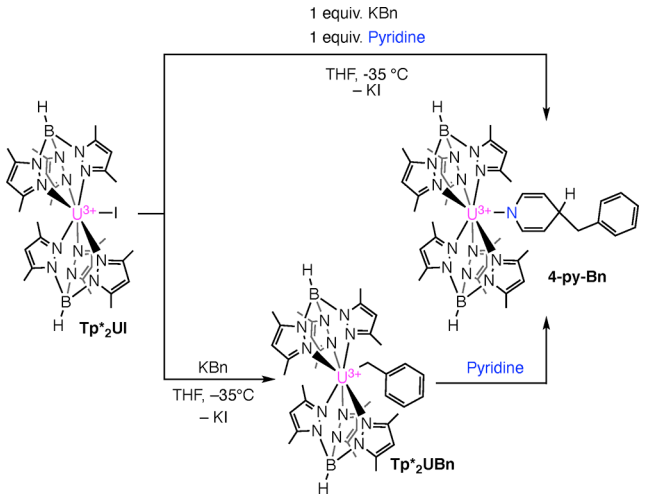

The absence of the three resonances beyond 20 ppm in the ^1H NMR spectrum and presence of the same three resonances in the ^2H NMR spectrum (δ in ppm (integration): A = 42.6 (2H), B = 27.9 (1H), and C = 22.8 (2H)) of an analogous synthesis with pyridine-d_5 (Figure 2) suggested the activation of pyridine and generation of **4-py-Bn-d_5**. The four resonances from 9 to 20 ppm (protons D, E, F, G) in the ^1H NMR spectrum of **4-py-Bn** displayed clear splitting into doublets and triplets. Such resolution in a paramagnetic NMR spectrum suggested that these resonances were derived from the benzyl group, which are further away from the paramagnetic uranium center than the activated pyridine.

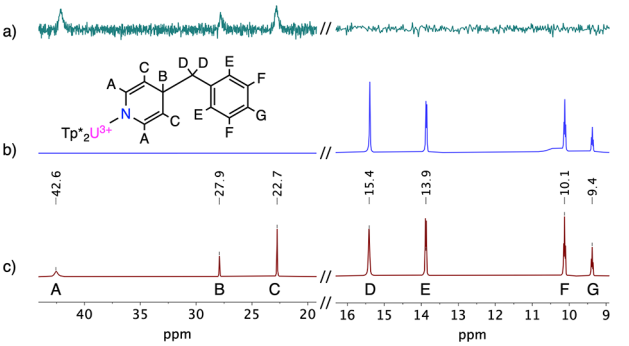

Figure 2. Paramagnetic NMR spectra: (a) ^2H NMR spectrum of **4-py-Bn-d_5** in C_6H_6. (b) ^1H NMR spectrum of **4-py-Bn-d_5** in C_6D_6. (c) ^1H NMR spectrum of **4-py-Bn** in C_6D_6. Their assignments to 4-py-Bn are also depicted as supported by a ^1H−^1H COSY NMR spectrum (Figure S21).

Blue-green **3-py-Si** and **4-py-Bn** both contain charge transfer bands at 570 and 630 nm as assessed by electronic absorption spectroscopy in THF solution. These bands are in contrast to **4-K**, which is bright orange due its absorption band at 450 nm.

https://doi.org/10.1021/acs.organomet.2c00633
Organometallics 2023, 42, 641−650

The NIR region for **3-py-Si** and **4-py-Bn** shows typical *f*–*f* transitions between 1150 to 1400 nm, also consistent with a U(III) oxidation state (Figure S31).[22,23] The infrared spectra for **3-py-Si** (2556, 2532 cm^{-1}) and **4-py-Bn** (2555, 2529 cm^{-1}) are typical for Tp* B–H bands in bis-Tp* U complexes.[23]

To establish if uranium is a necessity in the formation of the benzylpyridyl moiety, a control experiment was performed: addition of pyridine to a toluene solution of KBn resulted in an immediate color change from bright orange to yellow, generating [K][benzylpyridinide] *in situ*. [K(18-crown-6)][4-benzylpyridinide] (**4-K**) can be independently prepared and structurally characterized by sequestering the potassium cation with 18-crown-6 from the [K][benzylpyridinide] solution, revealing the 4-positional isomer of the benzylpyridinide anion (Scheme 3).

Scheme 3

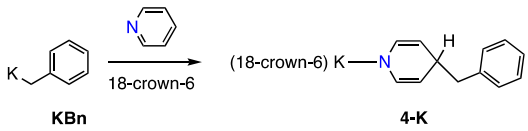

KBn **4-K**

The centers in compounds **3-py-Si** and **4-py-Bn** are distorted pentagonal bipyramids (Figure 3). The U–$N_{pyrazole}$ distances in **3-py-Si** and **4-py-Bn** are typical for bis-Tp* U(III) complexes as they range from 2.550(3)–2.733(3) and 2.554(4)–2.693(4) Å, respectively. The U–$N_{pyridine}$ distance in **3-py-Si** is 2.381(3) Å, while the U–$N_{pyridine}$ distance in **4-py-Bn** is between 2.371(11) and 2.38(2) Å (due to the disorder of the pyridyl moiety), all of which can be regarded as typical lengths for U(III)–N single bonds.[23]

In both **3-py-Si** and **4-py-Bn** (Figure 4, left), the N–C (N1–C1, N1–C5) and C–C bonds (C2–C3, C3–C4) lengthen while bonds C1–C2 and C4–C5 shorten. Both structures are in agreement with the bond metrics from Mazzanti's [K(2.2.2)-cryptand]$_2$ [{$(Me_3Si)_2N)_3U(III)$}$_2${μ-$(NC_5H_5)_2$}] complex and suggest dearomatization of the pyridine moiety.[14] In contrast, **4-K** shows a higher degree of aromaticity when compared to **3-py-Si** and **4-py-Bn** due to homogeneity of bond lengths, though can still be regarded as dearomatized when compared to free pyridine (Free pyridine: **C–N** = 1.336–1.347 Å, N–**C–C**–C = 1.381–1.393 Å, C–**C–C**–C = 1.378–1.389 Å).[37]

The angles about the 1- and 4-positions (N1 and C3 atoms bound non-H atoms) can be an indicator of hybridization at these two points (Figure 4, right). The sum of the angles surrounding N1 in **3-py-Si** (360.0(5)°) and in **4-py-Bn** (359.4(5)°) indicate near-planarity around N1. This planarity at the *N*-atom is structurally observed with other pyridyl-activated metal complexes (Table S6).[15−19,38−43] However, in **4-K** the sum of the angles surrounding N1 is 356.51°, showing that there is less planarity at this point which can be attributed to less π interaction between the nitrogen and potassium when compared to uranium. Likewise, the sums of the angles surrounding C3 in **3-py-Si**, **4-py-Bn**, and **4-K** (335.5(1)°, 330.6(1)°, and 330.98°, respectively) are also comparable to those found in the structures of most other pyridyl-activated metal complexes, which typically range from 331.0–360°.[15−19,38−43]

The root-mean-square (RMS) deviation from the least-squares planes can also be used as a planarity metric for the entire pyridyl moiety as a whole (an RMS deviation value of 0 is perfectly planar). These were calculated from the crystal structures for atoms N1, C1, C2, C3, C4, and C5 in both **3-py-Si**, **4-py-Bn**, and **4-K** (Figure 4, center). All pyridine moieties are near-planar, particularly **4-py-Bn** (0.0147), which is more planar than **4-K** (0.0218) likely due to partial conjugation along the C3–C6 and C6–C7 bonds, which permit C3 to have a slight sp^2-hybridized character. We note that this electronic effect is obscured by steric influence as seen with **3-py-Si** (0.0818) which does not allow for partial conjugation along the C–Si single bond, but does regard a larger distortion due to the larger substituent.

The geometry of the pyridyl ring can have a broad implication of the role of the sterics and electronics of the bound substrate in the 4-position. For example, the $(Me_3Si)_3Si$ ligand in **3-py-Si** is both a strong σ donor and sterically bulky which leads to a higher degree of planar distortion of the bound pyridine when compared to the benzyl group in **4-py-Bn**. However, the structure of **4-K** reveals that the identity of the metal plays a larger role in the C–N and C–C bond lengths of the pyridine ring, with stronger distortions caused by the bound uranium center in **3-py-Si** and **4-py-Bn**.

Mechanistic Insight. Based on the observed reactivity, it is hypothesized that addition of $(Me_3Si)_3SiK$ to Tp^*_2UI forms the product of salt metathesis, $[Tp^*_2U(III)Si(SiMe_3)_3]$, as a fleeting intermediate. The very reactive U–Si bond undergoes scission, and the Lewis basic solvents that are present are activated. The resulting products are those that satisfy the low-valent uranium ion's oxophilic tendencies, or need to have small, anionic (hard) donors, such as amides.

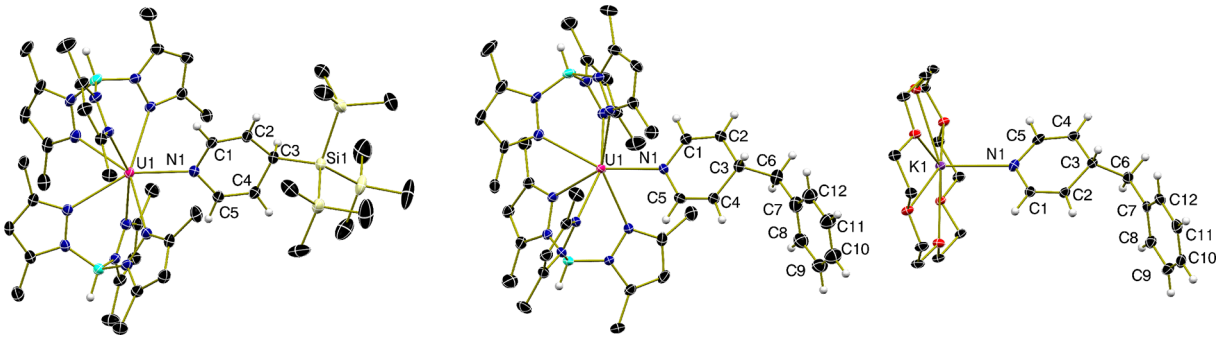

Figure 3. Molecular structures of **3-py-Si** (left), **4-py-Bn** (center), and **4-K** (right) displayed with 30% probability ellipsoids. Selected hydrogen atoms, solvent molecules, and minor disordered moieties were omitted for clarity.

https://doi.org/10.1021/acs.organomet.2c00633
Organometallics 2023, 42, 641–650

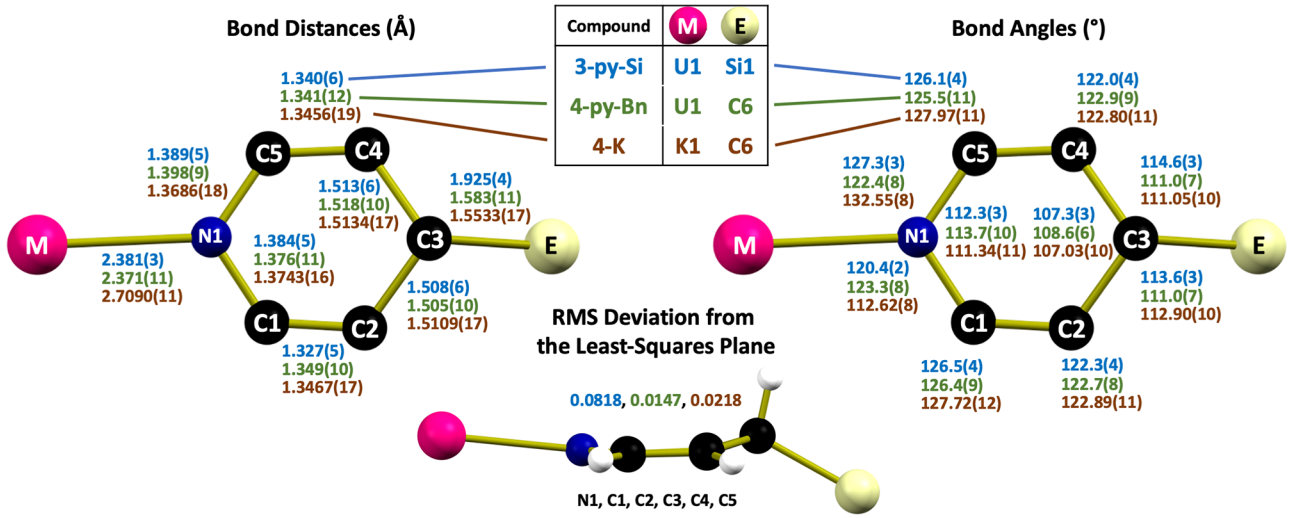

Figure 4. Bond distances (Å, top-down view, left), bond angles (degrees (deg), top-down view, right), and root-mean-square (RMS) deviation from the least-squares plane (side view, center) for the pyridine moiety in **3-py-Si** (blue values), **4-py-Bn** (green values), and **4-K** (brown values). Atoms N1, C1, C2, C3, C4, and C5 are used as the basis covariance matrix for calculating the least-squares mean plane. Atom colors are pink (**3-py-Si**: U1, **4-py-Bn**: U1, **4-K**: K1), blue (nitrogen), black (carbon), light yellow (**3-py-Si**: Si1, **4-py-Bn**: C6, **4-K**: C6), and white (hydrogen). The data for **4-py-Bn** are calculated using the major disordered moiety (67%). Selected hydrogen atoms and ligands are omitted for clarity.

In order to support this hypothesis, a series of control experiments were performed. Both $(Me_3Si)_3SiK{\cdot}2THF$ and $(Me_3Si)_3SiK{\cdot}2DME$ were found to be stable in solution for long periods of time; neither decomposes through a C−O bond cleavage pathway on their own.[30] This supports that the uranium ion is necessary to facilitate the solvent activation. When Tp^*_2UI is stirred in THF for long periods of time, in the absence of the potassium silyl reagent, C−O bond scission is also not observed, indicating that the silyl reagent is necessary for the product formation. Tp^*_2UI is also stable in DME for hours at ambient temperature, as judged by ^1H NMR spectroscopy. Thus, both uranium and the silyl reagent are necessary for the observed C−O bond activation.

Following these control experiments, it was found that when unsolvated $(Me_3Si)_3SiK$[44] is added to Tp^*_2UI in a non-Lewis basic solvent, such as toluene or C_6D_6, an intractable mixture of multiple paramagnetic products is observed through ^1H NMR spectroscopy, along with precipitation of KI. This supports that the formation of the U−Si bond is likely occurring, but is unstable and may easily decomposes under the reaction conditions.

The observed uranium-alkoxide products, **2-THF** and **2-DME**, were likely formed by σ bond metathesis at the U−Si bond with the Lewis basic solvents, resulting from a combination of both the greater oxophilicity of uranium vs silicon, and the steric bulk of Tp* hindering a strong interaction of the $(Me_3Si)_3Si-$ fragment with the uranium(III) ion. In the case of **2-DME**, formation of $(Me_3Si)_3SiMe$ is confirmed from ^1H and $^{29}Si\{^1H\}$ NMR spectroscopic analyses, and supports σ bond metathesis with a C−O bond in DME, resulting in transfer of $(Me_3Si)_3Si$ to the methyl group. Interestingly, neither Tp^*_2UOMe nor $(Me_3Si)_3SiCH_2CH_2OMe$ are observed in the ^1H or $^{29}Si\{^1H\}$ NMR spectra. It is possible that the bulky $(Me_3Si)_3Si-$ group prevents the internal DME C−O σ bond metathesis from occurring, thus leading to the formation of **2-DME** and $(Me_3Si)_3SiMe$. Although the $(Me_3Si)_3Si\cdot$ radical has been observed and even employed as a reducing agent and a functional group deprotector,[45] studies suggest the chemistry of $(Me_3Si)_3SiK$ and related silylpotassium species is dominated by two electron transformations.[30]

As observed with ethereal solvents, $(Me_3Si)_3SiK$ is also stable in pyridine with no reaction noted. When pyridine is used as the solvent for the addition of $(Me_3Si)_3SiK$ to Tp^*_2UI instead of an ethereal solvent, activation is noted with formation of **3-py-Si**, where the silyl group is added to the *para* position of the activated pyridine. In this case, however, no C−N bond is broken, supporting a divergent mechanism is occurring from that observed from ethereal solvents, likely a radical based one.

In the absence of isolating the U-Si species, support for pyridine activation by uranium(III) was gained by examining the reactivity of Tp^*_2UBn, an established U(III) alkyl. Stirring a solution of Tp^*_2UBn in pyridine for 1 h resulted in the formation of **4-py-Bn**, indicating the lack of stability of this benzyl compound in pyridine at room temperature. This supports pyridine activation at the *para* position, in analogy to the unstable U−Si bond as seen in **3-py-Si**. This result is similar to that previously seen when Tp^*_2UBn is treated with substituted triphenylphosphine oxides, ultimately generating $Tp^*_2U[OP(C_6H_5)_2(C_6H_5CH_2C_6H_5)]$, where the benzyl group is now in the *para* position of one of the phenyl rings.[26]

Using an excess of the hydrogen atom donors 1,4-cyclohexadiene (CHD) or 9,10-dihydroanthracene (DHA) in the synthesis of $Tp^*_2U[OP(C_6H_5)_2(C_6H_5CH_2C_6H_5)]$ produced no alteration in the ^1H NMR spectrum, indicating no H atom abstraction had occurred in either case. In this case, it was hypothesized that benzyl radical coupling to the *para*-position of triphenylphosphine oxide is faster than respective H atom abstraction or homocoupling. In the case of formation of **4-py-Bn**, the same observation was made. Treating a solution of Tp^*_2UBn in C_6D_6 with CHD or DHA and one equivalent of pyridine resulted in no disappearance of CHD or DHA with conversion to **4-py-Bn** noted in high yield. Thus, analogous chemistry to $Tp^*_2U[OP(C_6H_5)_2(C_6H_5CH_2C_6H_5)]$ is noted.

As in the case of triphenylphosphine oxide activation, it is likely that radical chemistry is occurring during pyridine activation. It is proposed that upon addition of pyridine to a

https://doi.org/10.1021/acs.organomet.2c00633
Organometallics 2023, 42, 641−650

solution of Tp^*_2UBn, pyridine association with the uranium(III) center facilitates benzyl radical dissociation. In concert, a putative $[Tp^*_2U]$ fragment reduces pyridine by one electron, which generates a radical in the *para* position by resonance. This then reacts with the extruded benzyl radical to form **4-py-Bn**. If benzyl radical loss happened prior to pyridine coordination, this would be evident from NMR experiments, and this was not observed. Furthermore, there was no evidence by ^{1}H NMR spectroscopy for the formation of bibenzyl or toluene during the course of the reaction, supporting that benzyl radical is subject to the cage effect,[46] where the it does not leave the coordination sphere of the uranium.

The idea of a radical pathway was further supported through KC_8 reduction of Tp^*_2UI in the presence of pyridine, presumably forming an equivalent of $[Tp^*_2U]$, which generates dimeric $[Tp^*_2U(NC_5H_5)]_2$ (**5-py-py**, Scheme 4).

Scheme 4

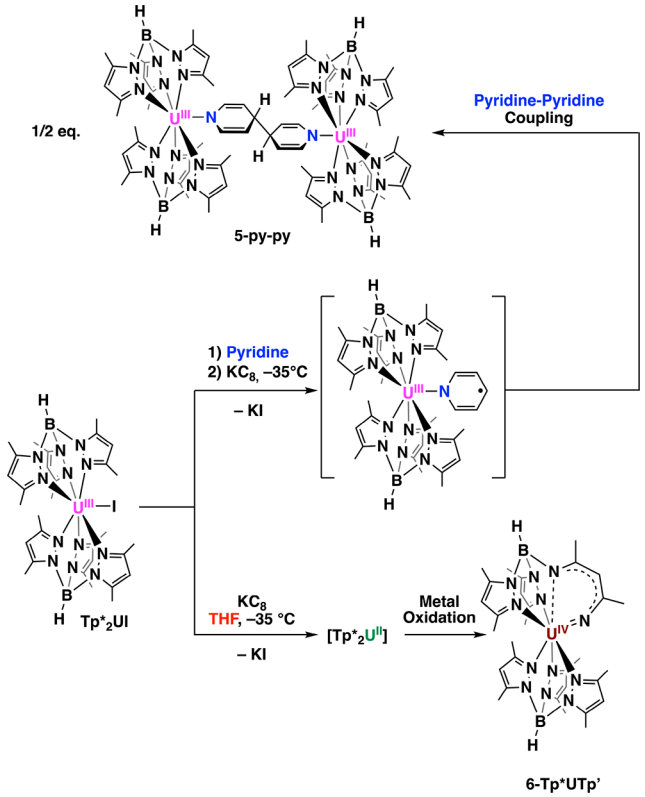

Preliminary single crystal diffraction data of **5-py-py** suggests C−C bond coupling between the pyridine moieties; however, the data quality is not precise enough to discern pyridine reduction through bond length analyses. Compound **5-py-py** appears structurally similar to other pyridine-coupled products.[14,15,17,19] The ^{1}H NMR spectrum shows broad resonances at 32.5, 44.3, and 47.6 ppm which suggest a similar pyridine activation to **3-py-Si** and **4-py-Bn** (Figure S23) and the ^{11}B{^{1}H} NMR correlates to U(III) (−7.3 ppm) (Figure S24).[23] The NIR region of the electronic absorption spectra strongly suggests U(III) and is nearly identical with that of **4-py-Bn** (Figure S31). Thus, **5-py-py** demonstrates that a uranium-pyridyl radical is a possible intermediate that can couple to the benzyl group.

A control experiment of the direct reduction of Tp^*_2UI with KC_8 in THF in the absence of pyridine resulted in formation of $Tp^*U^{IV}[(=NC(Me)C(H)-C(Me)N)B(H)(3,5\text{-dimethylpyrazole})_2]$ (**6-Tp*UTp′**, Scheme 4), which supports reductive N−N bond cleavage in one pyrazole ring of Tp* and oxidation of the uranium to U(IV). The ^{1}H NMR spectrum of **6-Tp*UTp′** has an asymmetric ligand set with distinct, sharp peaks, ranging from −48.59 to 81.65 ppm. Due to the complexity of this spectrum, the structural parameters were investigated by X-ray crystallography.

Needle-shaped yellow single crystals suitable for X-ray diffraction were grown from a concentrated solution of toluene and pentane (3:1) at −35 °C. Refinement of the data revealed a seven coordinate uranium ion in a pseudo trigonal prismatic geometry, with a traditionally coordinated κ^3-Tp* ligand as well as a new ligand derived from activation of a pyrazole group. While the bond distances are not reliable enough to be able to provide a meaningful discussion of their distances, we can see that one U−N bond is quite a bit shorter than the other, indicating multiple bond character, supporting a uranium(IV) ion by charge balance.

CONCLUSIONS

Attempting to synthesize uranium(III)-silyl bonds using the bis(Tp*) framework ultimately generated the isolable products of Lewis basic solvent activation. The wide range of NMR-active nuclei in these compounds enabled characterization by paramagnetic ^{1}H, ^{2}H, ^{11}B, and ^{29}Si NMR spectroscopy. Infrared spectroscopy and electronic absorption spectroscopy were used to identify and characterize these new uranium(III) derivatives as well, with the latter helping to corroborate the U(III) oxidation state of these derivatives. Structural data obtained from X-ray crystallography were collected and established activation of THF, DME, and pyridine. Mechanistic experiments were performed to determine under what conditions this activation chemistry occurs. The oxophilicity of uranium likely drives the activation of THF and DME to form strong U−O alkoxide bonds. A radical based mechanism is indicated in pyridine activation, as the formation of para-substituted pyridine is noted. In this case, the strong anionic U−N bond that resulted likely played a role in the observed activation chemistry. The instability of the proposed uranium−silicon bond in this study is mainly explained by the mismatch of hard uranium ions with softer main-group elements.

This study demonstrates that the electron rich uranium complexes readily activate accessible Lewis bases, giving trivalent products. This may have come from either a fleeting U−Si intermediate or from a reduced intermediate. This type of reactivity is important to establish for uranium, as trivalent actinides are a component of spent nuclear fuels, and ligand extraction represents an important separation technique. Uranium(III) is prone to disproportionation, but is not noted in this case, as no uranium(IV) products of Lewis base activation are observed, nor is decomposition to potential divalent uranium products. These studies represent unusual activation chemistry, as Lewis bases are known to support low valent uranium, rather than be activated by it. Further studies that encompass additional bases and their mechanisms of activation are ongoing.

EXPERIMENTAL SECTION

General Considerations. All air- and moisture-sensitive manipulations were performed using standard Schlenk techniques or using an MBraun inert atmosphere drybox with an atmosphere of purified nitrogen. The MBraun drybox was equipped with a cold well used for

https://doi.org/10.1021/acs.organomet.2c00633
Organometallics 2023, 42, 641−650

freezing samples with liquid nitrogen, dry ice and acetone baths, as well as two −35 °C freezers for cooling samples and crystallizing compounds. Solvents for sensitive manipulations including THF, toluene, and pentane were dried and deoxygenated using literature procedures with a Seca solvent purification system.[47] Pyridine was purified by stirring over CaH_2 for at least 2 days before distillation and stored over molecular sieves. 1,2-Dimethoxyethane (DME) was purified by stirring over CaH_2 for at least 2 days before distillation and stored over molecular sieves and sodium. THF-d_8 was purchased from Cambridge Isotope Laboratories (CIL) and stored over sodium in the glovebox freezer. Pyridine-d_5 was purchased from CIL, stirred over CaH_2, distilled, and stored over sieves. Benzene-d_6 (C_6D_6) was purchased from CIL, dried with molecular sieves and sodium, and degassed with six freeze−pump−thaw cycles. $(Me_3Si)_4Si$ was purchased from TCI, and KOtBu and 18-crown-6 were purchased from Sigma-Aldrich, and used without further purification. Tp*$_2$UI,[48] $(Me_3Si)_3SiK{\cdot}2THF$,[30] $(Me_3Si)_3SiK{\cdot}2DME$,[30] base-free $(Me_3Si)_3SiK$,[49] Tp*$_2$UBn,[20] and KBn[50] were synthesized using literature procedures. KC_8 was synthesized from a modified literature procedure.[51]

Caution! *U-238 is a weak α-emitter with a half-life of $t_{1/2} = 4 \times 10^9$ years. All manipulations were performed in an inert-atmosphere glovebox in a laboratory equipped with proper detection equipment.*

^{1}H NMR spectra were recorded on a Varian Inova 300 spectrometer operating at a frequency of 300 MHz or a Bruker AV400 spectrometer operating at a frequency of 400 MHz. All chemical shifts are reported relative to ^{1}H residual chemical shifts of benzene-d_6 (C_6D_6, 7.16 ppm) or THF-d_8 (1.72 ppm). For paramagnetic molecules, the ^{1}H NMR data are reported with the chemical shift, followed by the peak-width-at-half-height in Hertz, the integration value, and, where possible, the peak assignment. Multiplicities are assigned as singlet (s), doublet (d), triplet (t), or multiplet (m), and some moieties are abbreviated as trimethylsilyl (Me_3Si or $SiMe_3$), pyridinyl, (py) and benzyl (Bn). ^{11}B NMR spectra were recorded on a Varian Inova 300 spectrometer operating at a frequency of 96.24 MHz. ^{29}Si NMR spectra were recorded on a Bruker AV400 spectrometer operating at a frequency of 79.49 MHz and sometimes with the ^{29}Si INEPT pulse sequence.[52] Both ^{11}B and ^{29}Si NMR spectra are referenced to the deuterium signal. Solid state infrared spectra were recorded using a Thermo Nicolet 6700 spectrophotometer; samples were made by using KBr salt plates or a KBr pellet. Electronic absorption spectroscopic measurements were recorded at 294 K in sealed 1 cm quartz cuvettes with a Cary 6000i UV−vis−NIR spectrophotometer.

Single crystals suitable for X-ray diffraction of **1-THF**, **2-DME**, **3-py-Si**, **4-py-Bn**, **4-K**, and **5-py-py** were coated with poly(isobutylene) oil in the glovebox and quickly transferred to the goniometer head of a Bruker Quest diffractometer with a fixed chi angle, a sealed tube fine focus X-ray tube, single crystal curved graphite incident beam monochromator, a Photon II area detector and an Oxford Cryosystems low temperature device. Examination and data collection were performed with Mo Kα radiation (λ = 0.71073 Å) at 150 K. Single crystals suitable for X-ray diffraction of **6-Tp*UTp′** were coated with poly(isobutylene) oil in the glovebox and quickly transferred to the goniometer head of a Rigaku Rapid II diffractometer with a quarter chi circle and a 200 degree curved image plate detector at a fixed distance of 127.4 mm. Data for **6-Tp*UTp′** were collected using Cu Kα radiation (λ = 1.54184 Å) at 150 K.

Synthesis of $(Me_3Si)_3SiK{\cdot}2THF$. $(Me_3Si)_3SiK{\cdot}2THF$ was synthesized according to literature preparation.[30] In a 20 mL scintillation vial, $(Me_3Si)_4Si$ (1.00 g, 3.12 mmol) and KOtBu (1.05 equiv, 0.400 g, 3.27 mmol) were dissolved in 15 mL of THF. The light yellow solution darkened over the course of 16 h, which was then reduced in volume *in vacuo* to 1 mL. Pentane (10 mL) was added to the dark yellow solution and filtered into a clean vial to remove particulates. Colorless crystals were grown in the freezer at −35 °C over the course of a few hours in a 10:1 pentane/THF solution. The yellow mother liquor was decanted and the solids were further dried under a vacuum to yield $(Me_3Si)_3SiK{\cdot}2THF$ (1.094 g, 2.54 mmol, 90% yield). ^{1}H and ^{29}Si NMR data are concurrent with those found in the literature.[30]

Synthesis of $(Me_3Si)_3SiK{\cdot}THF$-d_8. A modified preparation of $(Me_3Si)_3SiK{\cdot}2THF$ was used to make the deuterated analog. In a 20 mL scintillation vial, $(Me_3Si)_4Si$ (0.200 g, 0.623 mmol) was combined with KOtBu (1.05 equiv, 0.080 g, 0.655 mmol). Then 0.5 mL of THF-d_8 was added to allow the solids to dissolve, turning the solution light yellow. After stirring at room temperature for 2 h, the volatiles were removed and the off-white solids were triturated with pentane. Placing the powder under a vacuum for 30 min afforded a flaky off-white powder that resembled $(Me_3Si)_3SiK{\cdot}2THF$.

Synthesis of $(Me_3Si)_3SiK{\cdot}2DME$. $(Me_3Si)_3SiK{\cdot}2DME$ was prepared according to literature preparation.[30] In a typical experiment, $(Me_3Si)_4Si$ (0.033g, 0.103 mmol) and KOtBu (0.013 g, 0.106 mmol) were combined as solids and dissolved in DME (4 mL). After stirring for 30 min, the volatiles were removed *in vacuo*, and replaced with pentane until the product was dry. Integration of the ^{1}H NMR spectrum revealed two molecules of DME for every $(Me_3Si)_3SiK$ molecule. The product was then used immediately in the synthesis of **2-DME**.

^{1}H NMR (C_6D_6, 300 MHz, 25 °C) δ (ppm) = 0.64 (s, 27H, $(Me_3Si)_3Si$), 2.95 and 2.97 (two singlets, 20H, DME CH_3 and CH_2).

Alternate Synthesis of $(Me_3Si)_3SiK{\cdot}2DME$. $(Me_3Si)_3SiK{\cdot}2DME$ can also be prepared by dissolving solid $(Me_3Si)_3SiK{\cdot}2THF$ in excess DME. The solution was dried and triturated with pentane to afford an off white powder which was used immediately in the synthesis of **2-DME**.

Synthesis of $(Me_3Si)_3SiK{\cdot}$pyridine. Colorless $(Me_3Si)_3SiK{\cdot}2THF$ (0.100 g, 0.232 mmol) was dissolved in pyridine. The volatiles were removed *in vacuo* and a second portion of pyridine was introduced. Pyridine was again removed and triturated with pentane affording an orange powder.

^{1}H NMR (C_6D_6, 300 MHz, 25 °C) δ (ppm) = 0.52 (s, 27H, $(Me_3Si)_3Si$), 6.76 (m, 2H, py 3,5-CH), 7.05 (m, 1H, py 4-CH), 8.37 (s, 2H, py 2,6-CH).

Synthesis of $(Me_3Si)_3SiK{\cdot}$pyridine-d_5. Colorless $(Me_3Si)_3SiK{\cdot}2THF$ (0.100 g, 0.233 mmol) was dissolved in minimal pyridine-d_5 and allowed to stir at room temperature for 1 h. The volatiles were removed *in vacuo* and a second minimal portion of pyridine-d_5 was introduced. Pyridine-d_5 was again removed under a vacuum for 30 min affording a flaky orange powder.

Synthesis of [K(18-crown-6)][4-benzylpyridinide] (4-K). To a THF (10 mL) solution of KBn (0.050 g, 0.384 mmol), pyridine (0.050 g, 0.633 mmol) was added causing a color change from orange to yellow. After stirring the yellow solution for 5 min, 18-crown-6 (0.101 g, 0.382 mmol) was added, the yellow solution took on a red color as it stirred for 10 min. After volatiles were removed *in vacuo* the powder was redissolved in THF (3 mL), and filtered into a clean vial to remove particulates. The concentrated THF solution was layered with pentane (6 mL) (1:2 THF/pentane) and left in the freezer. A crop of X-ray diffraction quality crystals of **4-K** were grown as large off-white needles in 34% yield (0.062 g, 0.132 mmol).

^{1}H NMR (C_6D_6, 300 MHz, 25 °C) δ (ppm) = 3.21 (s, 18-crown-6), 4.48 (m, Bn CH_2), 6.69 (m, py 3,5-CH), 6.65 (m, py 4-CH), 6.93−7.13 (m, Bn CH), 7.27 (m, Bn CH), 7.48 (m, Bn CH), 8.53 (m, py CH). FTIR (KBr Pellet, cm^{-1}) 3504, 3027, 2972, 2883, 2822, 2702, 2583, 2542, 1972, 1598, 1518, 1109, 962, 868, 704.

Synthesis of Tp*$_2$U[O(CH$_2$)$_4$Si(SiMe$_3$)$_3$] (1-THF). A solution of Tp*$_2$UI (0.050 g, 0.052 mmol) dissolved in 4 mL THF was cooled to −35 °C in the glovebox freezer. Then, $(Me_3Si)_3SiK{\cdot}2THF$ (0.022 g, 0.051 mmol) in 1 mL of THF was added slowly to the stirring solution. The purple solution momentarily developed a blue hue that quickly faded to a dark brown color. The stirring solution was allowed to warm to room temperature for 1 h. Volatiles were removed *in vacuo* and the green-brown solids were redissolved in pentane and filtered to remove KI salts. Removing pentane under a vacuum afforded **1-THF** as a brown powder in high yield (0.055 g, 0.048 mmol, 91.6% yield). Green-brown blocks of **1-THF** suitable for X-ray diffraction were grown from slow diffusion of pentane into a concentrated diethyl

https://doi.org/10.1021/acs.organomet.2c00633
Organometallics 2023, 42, 641−650

ether solution or precipitated from a concentrated pentane solution in the glovebox freezer.

^{1}H NMR (C_6D_6, 400 MHz, 25 °C) δ (ppm) = −11.14 (25, s, 9H, Tp* CH_3), −1.61 (5, s, 12H, Tp* CH_3), 3.86 (5, s, 27H, $(Me_3Si)_3Si$), 6.94 (8, s, 4H, Tp* CH), 13.67 (9, broad m, 2H, CH_2), 22.55 (13, broad m, 2H, CH_2), 43.03 (32, broad m, 2H, CH_2), 103.40 (69, broad m, 2H, CH_2). ^{11}B NMR (C_6D_6, 96.24 MHz, 25 °C) δ = −7.74 ppm (broad). ^{29}Si NMR (C_6D_6, 79.49 MHz, 25 °C) δ (ppm) = −8.6 (s, $(\underline{Me_3Si})_3Si$), −75.1 (s, $(Me_3Si)_3\underline{Si}$). FTIR (KBr Pellet, cm^{-1}) ν_{B-H} = 2561, 2562 cm^{-1}.

Synthesis of Tp*$_2$U[O(CH$_2$)$_2$OMe] (2-DME). In separate vials, Tp*$_2$UI (0.302 g, 0.314 mmol) and freshly synthesized $(Me_3Si)_3SiK$·2DME from $(Me_3Si)_3SiK$·2THF (0.135 g, 0.315 mmol) and DME (0.5 mL) were dissolved in toluene (4 mL in each vial) and cooled in the glovebox freezer to −35 °C. The solution of $(Me_3Si)_3SiK$·2DME was added slowly to the solution of Tp*$_2$UI and allowed to stir for 30 min before removing volatiles *in vacuo*. The brown residue was redissolved in minimal cold (−35 °C) pentane and filtered out as a pentane-insoluble product. Subsequent pentane washings of the brown precipitate at −35 °C gave **2-DME** in 47% yield (0.135 g, 0.149 mmol), which can be redissolved at room temperature and crystallized in minimal pentane or diethyl ether at −35 °C as diffraction quality brown blocks.

^{1}H NMR (C_6D_6, 400 MHz, 25 °C) δ (ppm) = −11.31 (46, s, 18H, Tp* CH_3), −1.8 (11, s, 18H, Tp* CH_3), 6.9 (10, s, 6H, Tp* CH), 10.4 (10, s, 3H, $OCH_2CH_2O\underline{CH_3}$), 43.3 (25, broad t, 2H, $OCH_2\underline{CH_2}OCH_3$), 100.6 (56, broad t, 2H, $O\underline{CH_2}CH_2OCH_3$). ^{11}B NMR ($C_6D_6$, 96.24 MHz, 25 °C) δ = −6.2 ppm (broad). FTIR (KBr Pellet, cm^{-1}) ν_{B-H} = 2550, 2527.

Synthesis of Tp*$_2$U[NC$_5$H$_5$-4-Si(SiMe$_3$)$_3$] (3-py-Si). A solution of Tp*$_2$UI (0.053 g, 0.055 mmol) dissolved in 2 mL toluene was cooled to −35 °C in the glovebox freezer. In a separate vial, $(Me_3Si)_3SiK$·pyridine (0.022 g, 0.54 mmol) was dissolved in 1 mL of toluene and cooled in the freezer. Then, the solution of $(Me_3Si)_3SiK$·pyridine was added slowly to the stirring Tp*$_2$UI solution. The purple mixture developed a green color and was allowed to stir for 1 h while warming to room temperature. Volatiles were removed *in vacuo* and the blue-green solids were redissolved in pentane and filtered. Removal of pentane from the blue-green solution under a vacuum afforded **3-py-Si** as a blue-green powder in moderate yield (0.044 g, 0.40 mmol, 69%). Green blocks of **3-py-Si** suitable for X-ray diffraction were grown from slow diffusion of pentane into a concentrated diethyl ether solution or precipitated from a concentrated pentane solution in the glovebox freezer.

^{1}H NMR (C_6D_6, 300 MHz, 25 °C) δ (ppm) = −2.37 (4, broad s, 1H, BH), 0.28 (2, s, 20H, Tp* CH_3), 5.11 (4, s, 27H, $(Me_3Si)_3Si$), 22.19 (12, s, 2H, 3-py CH), 32.73 (16, 1H, s, 4-py CH), 43.63 (21, s, 1H, 2-py CH). ^{11}B NMR (C_6D_6, 300 MHz, 25 °C) δ = −9.85 ppm (503, broad). ^{29}Si NMR (C_6D_6, 79.49 MHz, 25 °C) δ (ppm) = −6.8 (s, $(\underline{Me_3Si})_3Si$), −51.0 (s, $(Me_3Si)_3\underline{Si}$). FTIR (KBr Pellet) ν_{B-H} = 2556, 2532 cm^{-1}.

General Experimental Procedure for Equimolar Lewis Base Experiments with Tp*$_2$UI and (Me$_3$Si)$_3$SiK. In a 20 mL scintillation vial, a solution of Tp*$_2$UI (0.020 g, 0.021 mmol) dissolved in 0.5 mL C_6D_6 was frozen at −35 °C in the glovebox freezer. In a separate vial, 2 equiv of pyridine (0.003 g, 0.037 mmol) or 2 equiv of DME (0.004 g, 0.044 mmol) were added to a 0.5 mL C_6D_6 solution of $(Me_3Si)_3SiK$·2THF (0.009 g, 0.021 mmol) and frozen in the freezer. For the 1:1 DME:pyridine experiment, an appropriate amount of $(Me_3Si)_3SiK$·pyridine was synthesized and two equivalents of DME were added to this C_6D_6 solution. Then, the solution of $(Me_3Si)_3SiK$ was added slowly to the thawing Tp*$_2$UI solution. The solution was allowed to stir for 1 h while warming to room temperature. The 1 mL C_6D_6 solutions were filtered through Celite into a J-Young tube, spiked with approximately 2 μL of mesitylene as an internal standard (to assess relative amounts of product), sealed, and monitored through ^{1}H NMR spectroscopy (300 MHz, 25 °C).

1:1 THF:DME. Major product is **2-DME**. The ^{1}H NMR spectra for **1-THF** and **2-DME** are similar, but due to the absence of a large peak at 3.9 ppm and the presence of a large peak at 0.2 ppm, this was assigned to complete production of **2-DME**. **1-THF** was not observed.

1:1 THF:pyridine. Major product is **3-py-Si** along with other unidentified impurities. **1-THF** was not observed.

1:1 DME:pyridine. Major product is **3-py-Si** along with other unidentified impurities. **2-DME** was not observed.

Synthesis of Tp*$_2$U(NC$_5$H$_5$-4-Bn) (4-py-Bn). A 20 mL scintillation vial was charged with Tp*$_2$UI (0.036 g, 0.038 mmol), 2 mL of THF, and a stir bar. In a separate vial, pyridine (0.004 g, 0.052 mmol) was added to a solution of KBn (0.005 g, 0.054 mmol) in 1 mL of THF until the orange solution developed a yellow color. After cooling the solutions of Tp*$_2$UI and KBn in the glovebox freezer, the yellow solution was slowly added to the purple Tp*$_2$UI solution. The reaction mixture was stirred for 1 h while warming to room temperature, resulting in a green-blue solution. The volatiles were removed *in vacuo* and washed with pentane to afford a green-blue powder assigned as **4-py-Bn** (0.026 g, 0.026 mmol, 69% yield).

Alternate Synthesis of Tp*$_2$U(NC$_5$H$_5$-4-Bn) (4-py-Bn). A 20 mL scintillation vial was charged with Tp*$_2$UBn (0.030 g, 0.032 mmol), approximately 1 mL of pyridine, and a stir bar. The reaction mixture was stirred for 1 h at room temperature, resulting in a green-blue solution. The volatiles were removed *in vacuo* and washed with pentane 3 × 5 mL to afford a green-blue powder identified as **4-py-Bn** (0.027 g, 0.027 mmol, 82% yield). Single green crystals of **4-py-Bn** were grown from slow diffusion of pentane into a 1:1 THF/diethyl ether solution at −35 °C.

^{1}H NMR (C_6D_6, 300 MHz, 25 °C) δ (ppm) = 9.4 (4, t, 1H, J = 7 Hz, Bn *p*-CH), 10.2 (4, t, 2H, J = 7 Hz, Bn *m*-CH), 13.9 (5, d, 2H, J = 7 Hz, Bn *o*-CH), 15.4 (5, broad d, 2H, J = 4 Hz, CH_2), 22.8 (10, s, 3.3H, py 4-CH), 27.9 (17, s, 2.5H, py *m*-CH_2), 42.6 (96, s, 4H, py *o*-CH). ^{11}B NMR (C_6D_6, 96.24 MHz, 25 °C) δ = −10.0 ppm. FTIR (salt plate) ν_{B-H} = 2555, 2529 cm^{-1}.

Synthesis of [Tp*$_2$U(NC$_5$H$_5$)]$_2$ (5-py-py). A 20 mL scintillation vial was charged with Tp*$_2$UI (0.150 g, 0.156 mmol) and a stir bar then dissolved in 6 mL of toluene and approximately 0.5 mL of pyridine. After cooling the purple solution to −35 °C, KC_8 (0.022 g, 0.163 mmol, 1.1 equiv) was added to the Tp*$_2$UI solution as a solid and the mixture was allowed to stir overnight at ambient temperature. The dark blue mixture was then filtered through Celite in a medium frit removing green byproduct. The solids were then washed with pentane (3 × 5 mL) and **5-py-py** was extracted with THF (20 mL). Upon drying **5-py-py** was isolated as a blue powder in 72% yield (0.102 g, 0.056 mmol). Multiple crystallizations were attempted in concentrated solutions of THF, or slow diffusion or layering of pentane, diethyl ether, toluene, or C_6D_6 in a THF solution at −35 °C. Only concentrated THF solutions gave single crystals, although they did not give data suitable for bond analysis through X-ray diffraction. **5-py-py** decomposes in THF overnight at room temperature and is slightly soluble in aromatic solvents.

^{1}H NMR (C_6D_6, 300 MHz, 25 °C) δ (ppm) = 32.5 (14, s, 4H, py 3-CH), 44.3 (12, s, 2H, py 4-CH), 47.6 (2, s, py- 2-CH). ^{11}B NMR (THF-d_8, 96.24 MHz, 25 °C) δ = −7.3 ppm. FTIR (C_6D_6, salt plate) ν_{B-H} = 2550, 2523 cm^{-1}.

Synthesis of Tp*U(IV)[(═NC(Me)C(H)C(Me)N)B(H)(3,5-dimethylpyrazole)$_2$] (6-Tp*UTp′). A 20 mL scintillation vial was charged with Tp*$_2$UI (0.100g, 0.104 mmol), 3 mL of THF, and a stir bar. The purple solution was cooled to −35 °C in the glovebox freezer. Then, KC_8 (0.014 g, 0.104 mmol) was added as a solid to the stirring solution and the solution was allowed to stir for 1 h at ambient temperature. Volatiles were removed and the solids were introduced to pentane (4 × 5 mL) and filtered through a glass filter pipet. The resulting extract was dried to afford a yellow-brown powder in 32% yield (0.028 g, 0.034 mmol). Single crystals of **6-Tp*UTp′** were grown in a concentrated solution of toluene and pentane (3:1) in the glovebox freezer.

^{1}H NMR (C_6D_6, 25 °C): −48.59 (22, 6H, Tp*-CH_3), −41.07 (210, 1H, B−H), −20.49 (21, 3H, Tp*-CH_3), −13.50 (13, 6H, Tp*-CH_3), −12.49 (13, 6H, Tp*-CH_3), −11.63 (16, 2H, Tp*-CH), −4.32 (162, 1H, B−H), −1.15 (13, 2H, Tp*-CH), 17.63 (11, 6H, Tp*-

https://doi.org/10.1021/acs.organomet.2c00633
Organometallics 2023, 42, 641−650

CH_3), 52.83 (14, 1H, Tp*-CH), 70.94 (21, 3H, Tp*-CH_3−ring opened), 79.34 (24, 1H, Tp*-CH−ring opened), 81.65 (26, 3H, Tp*-CH_3−ring opened). FTIR (KBr pellet) ν_{B-H} = 2550, 2523 cm: 2476, 2549 cm^{-1} (B−H).

■ ASSOCIATED CONTENT

Supporting Information

The Supporting Information is available free of charge at https://pubs.acs.org/doi/10.1021/acs.organomet.2c00633.

Experimental details, spectroscopic characterization, and crystallographic data (PDF)

Accession Codes

CCDC 2208118−2208123 contain the supplementary crystallographic data for this paper. These data can be obtained free of charge via www.ccdc.cam.ac.uk/data_request/cif, or by emailing data_request@ccdc.cam.ac.uk, or by contacting The Cambridge Crystallographic Data Centre, 12 Union Road, Cambridge CB2 1EZ, UK; fax: +44 1223 336033.

■ AUTHOR INFORMATION

Corresponding Author

Suzanne C. Bart − *H. C. Brown Laboratory, Department of Chemistry, Purdue University, West Lafayette, Indiana 47907, United States;* orcid.org/0000-0002-8918-9051; Email: sbart@purdue.edu

Authors

Nathan J. Lin − *H. C. Brown Laboratory, Department of Chemistry, Purdue University, West Lafayette, Indiana 47907, United States*

Diana Perales − *H. C. Brown Laboratory, Department of Chemistry, Purdue University, West Lafayette, Indiana 47907, United States;* orcid.org/0000-0001-6885-9856

Ellen M. Matson − *H. C. Brown Laboratory, Department of Chemistry, Purdue University, West Lafayette, Indiana 47907, United States;* orcid.org/0000-0003-3753-8288

Matthias Zeller − *H. C. Brown Laboratory, Department of Chemistry, Purdue University, West Lafayette, Indiana 47907, United States;* orcid.org/0000-0002-3305-852X

Complete contact information is available at: https://pubs.acs.org/10.1021/acs.organomet.2c00633

Notes

The authors declare no competing financial interest.

■ ACKNOWLEDGMENTS

The X-ray crystallographic data in this work was obtained on instruments funded by the National Science Foundation through the Major Research Instrumentation Program under Grant CHE-1625543. The authors acknowledge a grant from the National Science Foundation (CHE-1665170).

■ REFERENCES

(1) Albrecht-Schmitt, T. E. Actinide Chemistry at the Extreme. *Inorg. Chem.* **2019**, *58* (3), 1721−1723.

(2) Barnea, E.; Eisen, M. S. Organoactinides in Catalysis. *Coord. Chem. Rev.* **2006**, *250* (7), 855−899.

(3) Fox, A. R.; Bart, S. C.; Meyer, K.; Cummins, C. C. Towards uranium catalysts. *Nature* **2008**, *455*, 341−349.

(4) Pace, K. A.; Klepov, V. V.; Berseneva, A. A.; Loye, H.-C. Covalency in Actinide Compounds. *Chem. Eur. J.* **2021**, *27* (19), 5835−5841.

(5) Narbutt, J. Chapter 24: Solvent Extraction for Nuclear Power. In *Liquid-Phase Extraction*; Poole, C. F., Ed.; Handbooks in Separation Science; Elsevier, 2020; pp 725−744. DOI: 10.1016/B978-0-12-816911-7.00024-4.

(6) Alwaeli, M.; Mannheim, V. Investigation into the Current State of Nuclear Energy and Nuclear Waste Management—A State-of-the-Art Review. *Energies* **2022**, *15* (12), 4275.

(7) Rupasinghe, D. M. R. Y. P.; Gupta, H.; Baxter, M. R.; Higgins, R. F.; Zeller, M.; Schelter, E. J.; Bart, S. C. Elucidation of Thorium Redox-Active Ligand Complexes: Evidence for a Thorium-Tri-(Radical) Species. *Inorg. Chem.* **2021**, *60* (18), 14302−14309.

(8) Jones, M. B.; Gaunt, A. J. Recent Developments in Synthesis and Structural Chemistry of Nonaqueous Actinide Complexes. *Chem. Rev.* **2013**, *113* (2), 1137−1198.

(9) Clark, D. L.; Sattelberger, A. P.; Bott, S. G.; Vrtis, R. N. Lewis Base Adducts of Uranium Triiodide: A New Class of Synthetically Useful Precursors for Trivalent Uranium Chemistry. *Inorg. Chem.* **1989**, *28* (10), 1771−1773.

(10) Avens, L. R.; Barnhart, D. M.; Burns, C. J.; McKee, S. D. Uranium-Mediated Ring Opening of Tetrahydrofuran. Crystal Structure of $UI_2(OCH_2CH_2CH_2CH_2I)_2(Ph_3P{=}O)_2$. *Inorg. Chem.* **1996**, *35*, 537−539.

(11) Boisson, C.; Berthet, J. C.; Lance, M.; Nierlich, M.; Ephirtikhine, M. Novel Ring-Opening Reaction of Tetrahydrofuran Promoted by a Cationic Uranium Amide Compound. *Chem. Commun.* **1996**, *18*, 2129−2130.

(12) Campello, M. P. C.; Domingos, Â.; Santos, I. Uranium Complexes with Hydrotris(Pyrazolyl) Borate. *J. Organomet. Chem.* **1994**, *484* (1), 37−46.

(13) Arunachalampillai, A.; Crewdson, P.; Korobkov, I.; Gambarotta, S. Ring Opening and C−O and C−N Bond Cleavage by Transient Reduced Thorium Species. *Organometallics* **2006**, *25* (16), 3856−3866.

(14) Modder, D. K.; Palumbo, C. T.; Douair, I.; Fadaei-Tirani, F.; Maron, L.; Mazzanti, M. Delivery of a Masked Uranium(II) by an Oxide-Bridged Diuranium(III) Complex. *Angew. Chem., Int. Ed.* **2021**, *60* (7), 3737−3744.

(15) Formanuik, A.; Ortu, F.; Liu, J.; Nodaraki, L. E.; Tuna, F.; Kerridge, A.; Mills, D. P. Double Reduction of 4,4′-Bipyridine and Reductive Coupling of Pyridine by Two Thorium(III) Single-Electron Transfers. *Chem.—Eur. J.* **2017**, *23* (10), 2290−2293.

(16) Labouille, S.; Nief, F.; Le Goff, X.-F.; Maron, L.; Kindra, D. R.; Houghton, H. L.; Ziller, J. W.; Evans, W. J. Ligand Influence on the Redox Chemistry of Organosamarium Complexes: Experimental and Theoretical Studies of the Reactions of $(C_5Me_5)_2Sm(THF)_2$ and $(C_4Me_4P)_2Sm$ with Pyridine and Acridine. *Organometallics* **2012**, *31* (14), 5196−5203.

(17) Lewis, R. A.; MacLeod, K. C.; Mercado, B. Q.; Holland, P. L. Geometric and Redox Flexibility of Pyridine as a Redox-Active Ligand That Can Reversibly Accept One or Two Electrons. *Chem. Commun.* **2014**, *50* (76), 11114−11117.

(18) Orr, S. A.; Kennedy, A. R.; Liggat, J. J.; McLellan, R.; Mulvey, R. E.; Robertson, S. D. Accessible Heavier S-Block Dihydropyridines: Structural Elucidation and Reactivity of Isolable Molecular Hydride Sources. *Dalton Trans.* **2016**, *45* (14), 6234−6240.

(19) Jaroschik, F.; Nief, F.; Le Goff, X.-F.; Ricard, L. Synthesis and Reactivity of Organometallic Complexes of Divalent Thulium with Cyclopentadienyl and Phospholyl Ligands. *Organometallics* **2007**, *26* (14), 3552−3558.

(20) Matson, E. M.; Forrest, W. P.; Fanwick, P. E.; Bart, S. C. Functionalization of Carbon Dioxide and Carbon Disulfide Using a Stable Uranium(III) Alkyl Complex. *J. Am. Chem. Soc.* **2011**, *133* (13), 4948−4954.

(21) Kraft, S. J.; Fanwick, P. E.; Bart, S. C. Synthesis and Characterization of a Uranium(III) Complex Containing a Redox-Active 2,2′-Bipyridine Ligand. *Inorg. Chem.* **2010**, *49* (3), 1103−1110.

(22) Perales, D.; Ford, S. A.; Salpage, S. R.; Collins, T. S.; Zeller, M.; Hanson, K.; Bart, S. C. Conversion of Trivalent Uranium Anilido to

Tetravalent Uranium Imido Species via Oxidative Deprotonation. *Inorg. Chem.* **2020**, *59* (17), 11910−11914.
(23) Perales, D.; Lin, N. J.; Bronstetter, M. R.; Ford, S. A.; Zeller, M.; Bart, S. C. Conversion of Uranium(III) Anilido Complexes to Uranium(IV) Imido Complexes via Hydrogen Atom Transfer. *Organometallics* **2022**, *41* (5), 606−616.
(24) Tatebe, C. J.; Zeller, M.; Bart, S. C. [2π+2π] Cycloaddition of Isocyanates to Uranium(IV) Imido Complexes for the Synthesis of U(IV) κ^2 -Ureato Compounds. *Inorg. Chem.* **2017**, *56* (4), 1956−1965.
(25) Perales, D.; Bhowmick, R.; Zeller, M.; Miro, P.; Vlaisavljevich, B.; Bart, S. C. Isolation of Uranium(III) Primary Phosphido Complexes. *Chem. Commun.* **2022**, *58* (69), 9630−9633.
(26) Tatebe, C. J.; Tong, Z.; Kiernicki, J. J.; Coughlin, E. J.; Zeller, M.; Bart, S. C. Activation of Triphenylphosphine Oxide Mediated by Trivalent Organouranium Species. *Organometallics* **2018**, *37* (6), 934−940.
(27) Réant, B. L. L.; Berryman, V. E. J.; Seed, J. A.; Basford, A. R.; Formanuik, A.; Wooles, A. J.; Kaltsoyannis, N.; Liddle, S. T.; Mills, D. P. Polarised Covalent Thorium(IV)− and Uranium(IV)−Silicon Bonds. *Chem. Commun.* **2020**, *56* (83), 12620−12623.
(28) Diaconescu, P. L.; Odom, A. L.; Agapie, T.; Cummins, C. C. Uranium−Group 14 Element Single Bonds: Isolation and Characterization of a Uranium(IV) Silyl Species. *Organometallics* **2001**, *20* (24), 4993−4995.
(29) Gransbury, G. K.; Réant, B. L. L.; Wooles, A. J.; Emerson-King, J.; Chilton, N. F.; Liddle, S. T.; Mills, D. P. Electronic Structure Comparisons of Isostructural Early D- and f-Block Metal(III) Bis(Cyclopentadienyl) Silanide Complexes. *Chem. Sci.* **2023**, *14* (3), 621−634.
(30) Marschner, C. A New and Easy Route to Polysilanylpotassium Compounds. *Eur. J. Inorg. Chem.* **1998**, *1998* (2), 221−226.
(31) Marsmann, H. C.; Raml, W.; Hengge, E. ^{29}Si-Kernresonanzmessungen an Polysilanen. 2. Isotetrasilane/^{29}Si NMR Measurements on Polysilanes. 2. Isotetrasilanes. *Z. Für Naturforschung B* **1980**, *35* (12), 1541−1547.
(32) Antunes, M. A.; Domingos, Â.; dos Santos, I. C.; Marques, N.; Takats, J. Synthesis and Characterization of Uranium(III) Compounds Supported by the Hydrotris(3,5-Dimethyl-Pyrazolyl)Borate Ligand: Crystal Structures of $[U(TpMe_2)_2(X)]$ Complexes (X= OC_6H_2-2,4,6-Me_3, Dmpz, Cl). *Polyhedron* **2005**, *24* (18), 3038−3045.
(33) Seaman, L. A.; Hrobárik, P.; Schettini, M. F.; Fortier, S.; Kaupp, M.; Hayton, T. W. A Rare Uranyl(VI)−Alkyl Ate Complex $[Li(DME)_{1.5}]_2[UO_2(CH_2SiMe_3)_4]$ and Its Comparison with a Homoleptic Uranium(VI)−Hexaalkyl. *Angew. Chem.* **2013**, *125* (11), 3341−3345.
(34) Hrobárik, P.; Hrobáriková, V.; Greif, A. H.; Kaupp, M. Giant Spin-Orbit Effects on NMR Shifts in Diamagnetic Actinide Complexes: Guiding the Search of Uranium(VI) Hydride Complexes in the Correct Spectral Range. *Angew. Chem., Int. Ed.* **2012**, *51* (43), 10884−10888.
(35) Windorff, C. J.; Evans, W. J. ^{29}Si NMR Spectra of Silicon-Containing Uranium Complexes. *Organometallics* **2014**, *33* (14), 3786−3791.
(36) Maria, P. C.; Gal, J. F. A Lewis Basicity Scale for Nonprotogenic Solvents: Enthalpies of Complex Formation with Boron Trifluoride in Dichloromethane. *J. Phys. Chem.* **1985**, *89* (7), 1296−1304.
(37) Mootz, D.; Wussow, H.-G. Crystal Structures of Pyridine and Pyridine Trihydrate. *J. Chem. Phys.* **1981**, *75* (3), 1517−1522.
(38) Hensen, K.; Lemke, A.; Stumpf, T.; Bolte, M.; Fleischer, H.; Pulham, C. R.; Gould, R. O.; Harris, S. Synthesis and Structural Characterization of (1,4−Dihydropyrid-1−Yl)Aluminum Complexes. *Inorg. Chem.* **1999**, *38* (21), 4700−4704.
(39) Huang, W.; Khan, S. I.; Diaconescu, P. L. Scandium Arene Inverted-Sandwich Complexes Supported by a Ferrocene Diamide Ligand. *J. Am. Chem. Soc.* **2011**, *133* (27), 10410−10413.
(40) Dugan, T. R.; Bill, E.; MacLeod, K. C.; Christian, G. J.; Cowley, R. E.; Brennessel, W. W.; Ye, S.; Neese, F.; Holland, P. L. Reversible C−C Bond Formation between Redox-Active Pyridine Ligands in Iron Complexes. *J. Am. Chem. Soc.* **2012**, *134* (50), 20352−20364.
(41) Jochmann, P.; Dols, T. S.; Spaniol, T. P.; Perrin, L.; Maron, L.; Okuda, J. Insertion of Pyridine into the Calcium Allyl Bond: Regioselective 1,4-Dihydropyridine Formation and C−H Bond Activation. *Angew. Chem., Int. Ed.* **2010**, *49* (42), 7795−7798.
(42) Lemmerz, L. E.; Spaniol, T. P.; Okuda, J. 1,4-Dihydropyridyl Complexes of Magnesium: Synthesis by Pyridine Insertion into the Magnesium−Silicon Bond of Triphenylsilyls and Catalytic Pyridine Hydrofunctionalization. *Dalton Trans.* **2018**, *47* (36), 12553−12561.
(43) Lichtenberg, C.; Spaniol, T. P.; Perrin, L.; Maron, L.; Okuda, J. Reversible 1,4-Insertion of Pyridine Into a Highly Polar Metal−Carbon Bond: Effect of the Second Metal. *Chem. Eur. J.* **2012**, *18* (21), 6448−6452.
(44) Kayser, C.; Fischer, R.; Baumgartner, J.; Marschner, C. Tailor-Made Oligosilyl Potassium Compounds. *Organometallics* **2002**, *21* (6), 1023−1030.
(45) Chatgilialoglu, C.; Lalevée, J. Recent Applications of the $(TMS)_3SiH$ Radical-Based Reagent. *Molecules* **2012**, *17* (1), 527−555.
(46) Turro, N. J.; Chow, M.-F.; Chung, C.-J.; Tanimoto, Y.; Weed, G. Time-Resolved Laser Flash Spectroscopic Study of Benzyl Radical Pairs in Micelle Cages. *J. Am. Chem. Soc.* **1981**, *103* (15), 4574−4576.
(47) Pangborn, A. B.; Giardello, M. A.; Grubbs, R. H.; Rosen, R. K.; Timmers, F. J. Safe and Convenient Procedure for Solvent Purification. *Organometallics* **1996**, *15* (5), 1518−1520.
(48) Sun, Y.; McDonald, R.; Takats, J.; Day, V. W.; Eberspacher, T. A. Synthesis and Structure of Bis[Hydrotris(3,5-Dimethylpyrazolyl)-Borato]Iodouranium(III), $U[HB(3,5\text{-}Me_2Pz)_3]_2I$: Unprecedented Side-On Interaction Involving a Hydrotris(Pyrazolyl)Borate Ligand. *Inorg. Chem.* **1994**, *33* (20), 4433−4434.
(49) Niemeyer, M. Reactions of Hypersilyl Potassium with Rare-Earth Metal Bis(Trimethylsilylamides): Addition versus Peripheral Deprotonation. *Inorg. Chem.* **2006**, *45* (22), 9085−9095.
(50) Johnson, S. A.; Kiernicki, J. J.; Fanwick, P. E.; Bart, S. C. New Benzylpotassium Reagents and Their Utility for the Synthesis of Homoleptic Uranium(IV) Benzyl Derivatives. *Organometallics* **2015**, *34* (12), 2889−2895.
(51) Chakraborty, S.; Chattopadhyay, J.; Guo, W.; Billups, W. E. Functionalization of Potassium Graphite. *Angew. Chem.* **2007**, *119* (24), 4570−4572.
(52) Blinka, T. A.; Helmer, B. J.; West, R. Polarization Transfer NMR Spectroscopy for Silicon-29: The INEPT and DEPT Techniques. *Adv. Organomet. Chem.* **1984**, *23*, 193−218.

https://doi.org/10.1021/acs.organomet.2c00633
Organometallics 2023, 42, 641−650